The International Journal of Advanced Manufacturing Technology (2024) 132:5005–5016
https://doi.org/10.1007/s00170-024-13663-z

ORIGINAL ARTICLE

Mathematical model of non-generated straight bevel gears based on a four-axis CNC machine

Yi-Pei Shih[1] · **Guang-Yu Chen**[1]

Received: 2 February 2024 / Accepted: 17 April 2024 / Published online: 28 April 2024

Abstract
High-precision straight bevel gears are commonly manufactured using the generating method, which requires specialized equipment such as a dedicated or five-axis CNC machine for mass production. While the existing forming process can also be applied to produce SBGs, which offers a more cost-effective solution with a four-axis CNC machine, it results in inferior gear contact performance. This paper introduces a novel forming (non-generating) method. The goal is to enhance the gear contact performance. First, the tool profile of the pinion is computed based on the ring gear's conjugate tooth surface. Subsequently, a sensitivity analysis on the tooth surface, considering four-axis motion coefficients, facilitates the calculation of correction amounts for tooth cutting motion. This process determines the pinion's tooth surface, optimizing the contact performance by ensuring it contacts the ring gears precisely at a point. Ease-off and tooth contact analyses are utilized to evaluate the contact performance of the designed gear pair. Furthermore, VERICUT software is employed for cutting simulation to validate the NC machining codes. After this, a cutting experiment is conducted to verify the correctness of our mathematical model.

Keywords Straight bevel gears · Forming method · Non-generating · Four-axis CNC machine · VERICUT

1 Introduction

Straight bevel gears (SBGs) are conical in shape with straight teeth that transmit power between two intersecting axes under low speed. They are widely applied in many fields, such as differentials (vehicles), gear reducers, industrial machinery, and heavy machinery. In the design of high-precision SBGs, meeting the meshing conditions of spatial surfaces is indispensable. The theoretical tooth surface may exhibit slight variations depending on the design and the specific cutting methods. However, compared to other members of the bevel gear family, SBGs possess the advantage of having a simpler shape, rendering them relatively easy to manufacture. The conventional cutting methods for SBGs are generally classified into two categories: the generating and forming (non-generating) methods. The generating method usually employs a straight-edged tool in reciprocating or rotating milling motion to simulate the generation of a tooth on an imaginary generating gear. This imaginary generating gear is then fixed to a cradle table, and the cradle table and workpiece roll for the generating motion.

The mass-production generating methods can be implemented in two ways, including (1) the two-tool generating method and (2) the Coniflex cutting method with two giant interlocked circular cutters [1]. Both of the generating methods require dedicated machines to implement the generating process. As for the forming methods, three common ways are applied, including (1) the milling method with a disk tool [2], (2) the template planning tooth method, and (3) the Revacycle method with a large circular-type cutter [3]. The first method only requires a four-axis CNC machine; however, it will produce gears with poorer contact performance. The latter two methods require dedicated machines. The gear pairs produced by forming methods have lower contact performance than those by generating methods because the latter have point-conjugated tooth surfaces. If a gear pair has a reduction ratio greater than four, the ring gear is often processed using a forming method, while the pinion is processed using a generating method. The error of the ring gear's tooth surfaces can be compensated for on the tooth surface of the pinion. However, the generating method uses

✉ Yi-Pei Shih
shihyipei@mail.ntust.edu.tw

[1] Department of Mechanical Engineering, National Taiwan University of Science and Technology, No. 43, Sec. 4, Keelung Rd., Taipei 106335, Taiwan, Republic of China

five degrees of freedom in motion. Therefore, a dedicated machine or an expensive five-axis machine is required.

Among the various methods available, the disk milling cutting method is a good choice for producing large-size SBGs because it utilizes simple disk milling techniques and the widespread availability of four-axis machines. However, the conventional approach frequently encounters challenges associated with inadequate contact performance within the gear pair. Manufacturers typically rely on trial-and-error methods to adjust the pinion's tool profile and NC codes for enhanced gear performance. Unfortunately, this iterative process is to be time-consuming.

Many researchers have established the mathematical models of SBGs depend on diverse cutting methods. In the early stages, Ichino et al. [4] proposed the tooth surface generated by a quasi-complementary crown gear. Chang and Tsay [5] developed a mathematical model for SBGs with the octoid form and investigated their tooth contact analysis and tooth undercutting. Machines employ both methods, necessitating a cradle for the generating process. Özel et al. [6] used end mills to cut SBGs, while Tsuji et al. [7] employed end mills to manufacture large-sized SBGs on a multitasking machine. Wang [8] introduced an envelope-shaping method for producing large-sized SBGs. These three methods can be implemented on three-axis to five-axis milling machines. However, they are time-consuming due to the necessity of contour machining. Coniflex SBGs have crowning of the teeth, exhibiting excellent contact performance. Furthermore, this approach can serve as a grinding process for producing highly precise gears, rendering it a widely adopted method for mass production. Stadtfeld [9] proposed a CNC free-form machine to replace dedicated machines for manufacturing the Coniflex SBGs. Zhang et al. [10] developed their machine and mathematical model for the Coniflex SBGs. Shih et al. [11] establish their mathematical model of the Coniflex SBGs based on the five-axis CNC machine. After that, they [12] found the mathematical model of the Gleason straight-bevel Coniflex generator. Based on the provided model, modern numerical methods can be applied to conduct tooth contact analysis and reduce gear manufacturing errors. Fuentes-Aznar et al. [13] presented their mathematical model for the Coniflex SBGs and investigated the influence of the tool radius on bending stresses using the finite element method. The methods mentioned above involve single indexing using a milling process. Continuous indexing has recently attracted attention due to its relatively fast processing speed and accuracy. Shih proposed [14] the mathematical model of face-hobbed SBGs. Subsequently, her research team [15] conducted this cutting method on a six-axis CNC bevel gear cutting machine. Li et al. [16] developed a cycloid rotational indexing method for SBGs. Most existing mass-production methods are conducted on specialized dedicated machines, six-axis CNC bevel gear cutting machines, or five-axis CNC milling machines. In contrast, four-axis CNC machine tools are more affordable and accessible. However, a four-axis method for manufacturing SBG gears with optimal contact performance has not yet been developed.

This paper aims to develop a mathematical model for SBGs based on a four-axis CNC milling machine. The gears are manufactured using the forming method, exhibiting commendable contact performance. The design of the pinion's tooth surface uses the application of an ease-off technique. Initially, the ring gear serves as the reference gear, and the profile of the disk tool for the pinion is derived based on the gear's conjugate tooth surface. After this, a sensitivity analysis method is utilized to determine the corrections required for the four-axis motion during the cutting process of the pinion. The contact performance of the design gear pair is evaluated using ease-off and tooth contact analysis. The resulting numerical control (NC) codes are then programmed and simulated using VERICUT software. Finally, a cutting experiment is executed to validate the correctness of our developed mathematical model.

2 Mathematical model of the gear tooth surface based on a universal machine

When the ratio of teeth numbers in a gear pair is greater than four, the ring gear in the gear pair can be manufactured using the forming method. In this case, the pinion must be processed using the generating method to achieve conjugate contact between two gears. During processing, the forming method usually adopts a disk tool. The tool's outer edge is tangent to the gear tooth root line. The tool moves from the toe to the heel of the gear to produce the entire tooth surface. Figure 1 depicts the coordinate systems between a disk tool and the work gear based on a universal machine for manufacturing a gear. The tool and the work gear connect fixedly to coordinate systems S_t and S_1, respectively, while the auxiliary coordinate

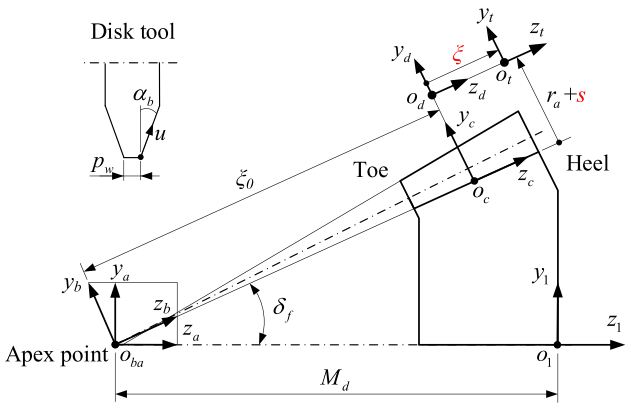

Fig. 1 Coordinate systems between a disk tool and the work gear are based on a universal machine

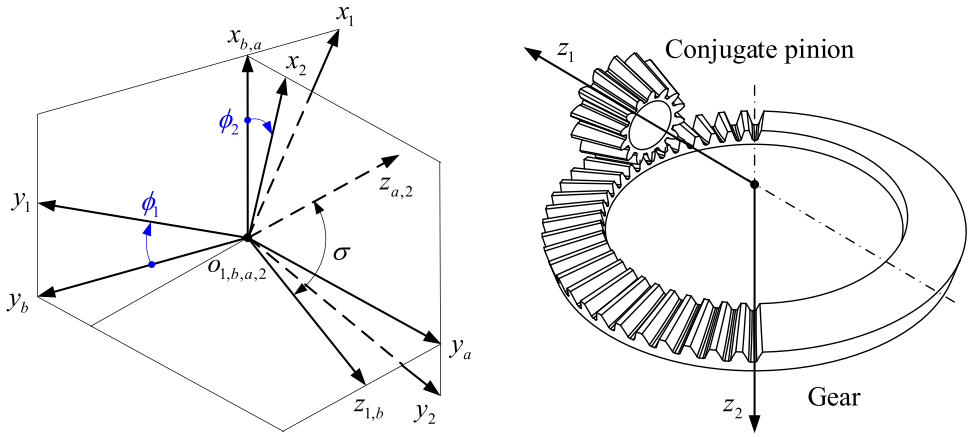

Fig. 2 Coordinate systems between the ring gear and its conjugate pinion

systems S_a to S_d indicate the relative motion between them. Where the gear parameter δ_f is the gear's root angle, M_d is the mounting distance, and ξ_0 is the cone distance at the mean. The parameter ξ is a variable controlling the infeed from gear toe to heel and s is the cutting stock.

The tool profile for machining the ring gear is directly specified, while the pinion's tool profile needs to be further determined based on the gear's tooth surface. The tool's cutting edge of the ring gear can be either a straight or circular edge, both with a fillet. The former's position vector may be represented in the tool coordinate system S_t as

$$\mathbf{r}_t(u,\beta) = \left[x\ \left(y - r_a\right)cos\ \beta - \left(y - r_a\right)sin\ \beta\ 1\right]^T \tag{1}$$

here

$$\begin{cases} x = \pm\left(p_w/2 + usin\alpha_b\right) \\ y = ucos\alpha_b \end{cases}$$

where u is the profile variable of the cutting edge, β is the tool's rotation angle, α_b is the profile angle, p_w is the point width, and r_a is the tool radius. The tool locus position vector $\mathbf{r}_1$ observed in S_1 is represented as Eq. (2) through a coordinate transformation matrix from S_t to S_1.

$$\mathbf{r}_1(u,\beta,s,\xi) = \mathbf{M}_{1t}(s,\xi)\mathbf{r}_t(u,\beta) \tag{2}$$

where the transformation matrix is

$$\mathbf{M}_{1t}(s,\xi) = \begin{bmatrix} 1 & 0 & 0 & 0 \\ 0 & cos\delta_f & sin\delta_f & 0 \\ 0 & -sin\delta_f & cos\delta_f & -M_d \\ 0 & 0 & 0 & 1 \end{bmatrix} \begin{bmatrix} 1 & 0 & 0 & 0 \\ 0 & 1 & 0 & r_a + s \\ 0 & 0 & 1 & \xi_0 + \xi \\ 0 & 0 & 0 & 1 \end{bmatrix}$$

The final tooth surface can be obtained when the cutting stock s equals zero. Finally, adhering to the conjugate condition where the normal $\mathbf{n}_1$ is perpendicular to the relative velocity $\mathbf{v}_1^{(1t)}$, the following meshing equation [17] can be employed to ascertain the tooth surface of the gear.

$$f_1(u,\beta,\xi) = \mathbf{n}_1 \cdot \mathbf{v}_1^{(1t)} = \left[\frac{\partial \mathbf{r}_1(u,\beta,\xi)}{\partial u} \times \frac{\partial \mathbf{r}_1(u,\beta,\xi)}{\partial \beta}\right] \cdot \left[\frac{\partial \mathbf{r}_1(u,\beta,\xi)}{\partial \xi}\ \dot{\xi}\right] = 0 \tag{3}$$

3 Design a tool profile of the pinion

Designing the gear teeth to promote point contact on the tooth surfaces between two mating gears is a common practice to enhance the meshing performance of bevel gears. In this context, the pinion undergoes manufacturing through the forming

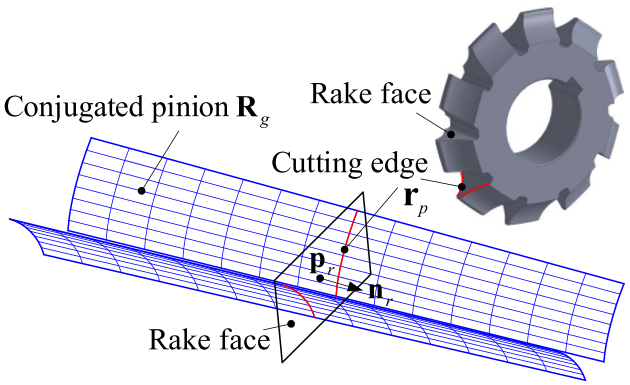

Fig. 3 Profile of a disk tool for the pinion

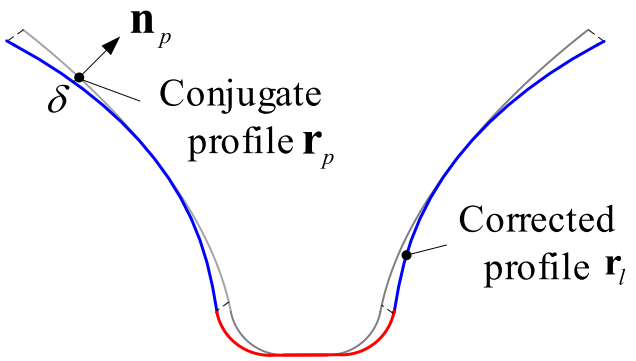

Fig. 4 Profile crowning of the disk tool for the pinion

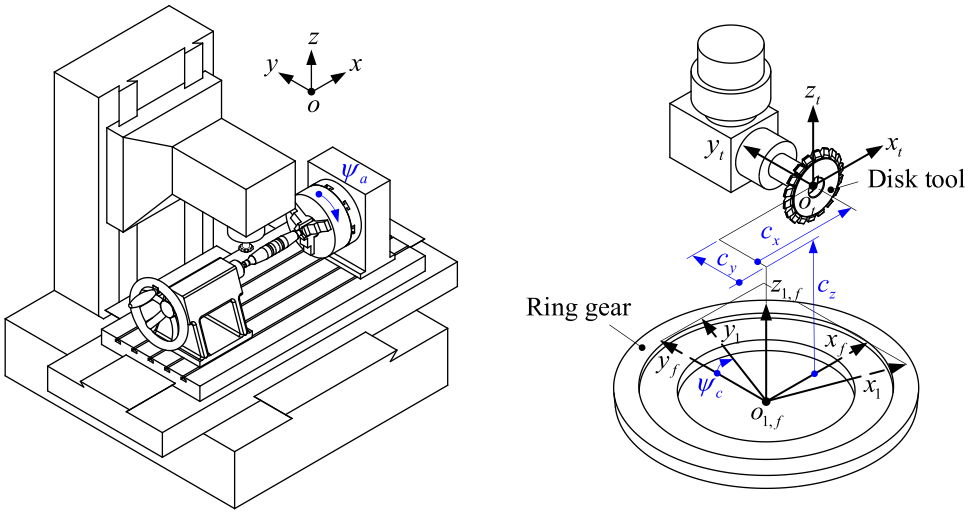

(a) Four-axis CNC machine for the pinion (b) Coordinate systems for the ring gear

Fig. 5 Coordinate systems between the disk tool and the work gear for the four-axis CNC machine

method instead of the generating method. Initially, the profile of the disk tool must be designed. The tool profile for the pinion is determined by referencing the conjugate tooth surface of the ring gear. We can use the ring gear as a tool to cut the pinion, thus obtaining tooth surfaces that are conjugate with the ring gear. The pinion and gear are installed in their respective assembly positions as shown in Fig. 2. They are fixedly connected to coordinate systems S_1 and S_2, respectively. The auxiliary coordinate systems S_a and S_b describe the assembly position between them, where the parameters ϕ_1 and ϕ_2 are the rotation angles of the pinion and gear, respectively, and σ is their shaft angle.

Assuming that $\mathbf{R}_2$ is the position of the gear's tooth surface having two independent variables, u and β, its locus position in S_1 can be represented as

$$\mathbf{r}_g(u,\beta,\phi_1,\phi_2) = \mathbf{M}_{12}(\phi_1,\phi_2)\mathbf{R}_2(u,\beta) \tag{4}$$

The coordinate transformation matrix is

$$M_{12}(\phi_1,\phi_2) = \begin{bmatrix} \cos\phi_1 & -\sin\phi_1 & 0 & 0 \\ \sin\phi_1 & \cos\phi_1 & 0 & 0 \\ 0 & 0 & 1 & 0 \\ 0 & 0 & 0 & 1 \end{bmatrix} \begin{bmatrix} 1 & 0 & 0 & 0 \\ 0 & \cos\sigma & -\sin\sigma & 0 \\ 0 & \sin\sigma & \cos\sigma & 0 \\ 0 & 0 & 0 & 1 \end{bmatrix} \begin{bmatrix} \cos\phi_2 & -\sin\phi_2 & 0 & 0 \\ \sin\phi_2 & \cos\phi_2 & 0 & 0 \\ 0 & 0 & 1 & 0 \\ 0 & 0 & 0 & 1 \end{bmatrix}$$

In the above equation, the ratio of ϕ_1 to ϕ_2 is equal to z_2/z_1, where z_1 and z_2 represent the teeth numbers of the pinion and gear, respectively. Consequently, the locus becomes a function of two tool variables, u and β, along with one motion variable ϕ_2. The conjugate tooth surface $\mathbf{R}_g$ can be determined by the following equation of meshing:

$$f_g(u,\beta,\phi_2) = \mathbf{n}_g \cdot \mathbf{v}_g^{(g2)} = \left[\frac{\partial \mathbf{r}_g(u,\beta,\phi_2)}{\partial u} \times \frac{\partial \mathbf{r}_g(u,\beta,\phi_2)}{\partial \beta}\right] \cdot \left[\frac{\partial \mathbf{r}_g(u,\beta,\phi_2)}{\partial \phi_2}\dot{\phi}_2\right] = 0 \tag{5}$$

Following this, by defining the tool's rake face at the midpoint of the conjugate tooth surface, the intersection curves $\mathbf{r}_p$ can be determined using Eq. (6), where $\mathbf{p}_r$ represents a point on the plane, and $\mathbf{n}_r$ is the normal vector to the plane. Subsequently, the normal $\mathbf{n}_p$ to the curve can be determined. These curves collectively shape the contour of the tool, as illustrated in Fig. 3.

$$\mathbf{n}_r \cdot \left(\mathbf{R}_g(u,\beta) - \mathbf{p}_r\right) = 0 \tag{6}$$

Considering assembly and manufacturing errors, gear pairs are typically designed for point contact. This necessitates fine-tuning the pinion's tooth surface along profile and longitudinal directions. A specialized tool achieves profile crowning, while longitudinal crowning is incorporated

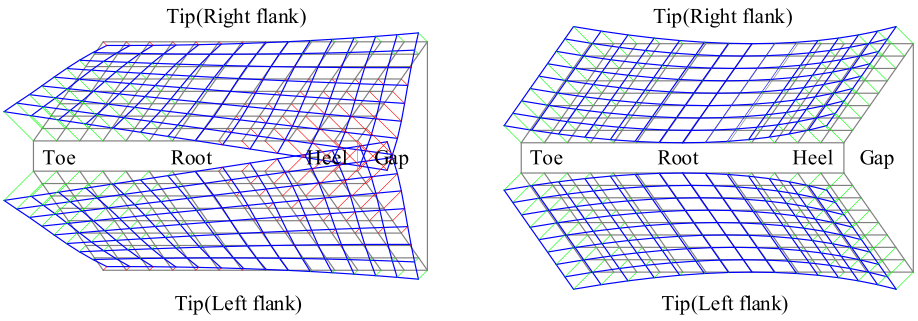

(a) Deviations δ_e compared to the conjugated surface (b) Longitudinal crowning δ_c

Fig. 6 Target corrections for the pinion's tooth surface

Table 1 Basic gear, gear blank, and tool parameters for the example pair

Items		Pinion		Ring gear
(A) Basic gear data				
Number of teeth	z	13		153
Outer module	m_n		3.000	
Pressure angle	α_n		20.000°	
Shaft angle	σ		90.000°	
Backlash at mean point	B		0.100	
(B) Gear blank data				
Pitch angle	δ	4.857°		85.143°
Face angle	δ_a	5.662°		85.659°
Root angle	δ_f	4.341°		83.886°
Outer diameter	d_{ae}	39.000		459.000
Outer whole depth	h_e	6.264		6.564
Face width	b		38.000	
Mounting distance	M_d	230.500		43.500
(C) Disk tool data				
Radius of the disk tool	r_a	32.500		63.000
Pressure angle	α_b	20.000°		20.000°
Initial point width	p_{w0}	2.200		2.040
Fillet radius	ρ_b	0.900		0.800
Relief amount, max	δ_{max}	0.030		–

during machining. A second-order correction is applied to the tool profile for the profile points depicted in Fig. 4. Utilizing Eq. (7), we subsequently employ a fourth-degree polynomial to fit the corrected profile points $\mathbf{r}_l$, as outlined in Eq. (8), where δ represents the correction quantity. This modified tool is then employed to generate the initial tooth surfaces of the pinion by the aforementioned mathematical model.

$$\mathbf{r}_l = \mathbf{r}_p - \delta \mathbf{n}_p \tag{7}$$

$$\mathbf{r}_l(u) = \sum_{k=0}^{4} a_k u^k \tag{8}$$

4 Four-axis coordinates for manufacturing SBGs

Both the pinion and gear undergo machining for their tooth surfaces utilizing a standard four-axis milling machine. Four-axis centers can achieve up to 4-axis simultaneous machining by programming numerical control (NC) programs. They offer great flexibility, particularly in applications related to machining tooth surfaces. Figure 5 illustrates the coordinate systems between the disk tool and the work gear on the four-axis machine. To facilitate the machining of the pinion, a workpiece rotary table is situated on the machine bed, allowing the pinion workpiece to be horizontally positioned. An additional 90° tool axis is installed for the ring gear, as depicted in the diagram.

Transforming the tool origin from the coordinate system S_t to S_l by the transformation matrix $\mathbf{M}_{lt}(s, \xi)$ in Eq. (2) yields the tool cutting coordinates, as shown in Eq. (9), where variables s and ξ are used to control the cutting stock and the infeed from toe to heel of the tooth surface. The workpiece rotation angle for the pinion is around the A-axis, the X- and Y-axes are employed for motion along the face width, and the Z-axis is used to position the tool at the cutting location. In the ring gear's case, the workpiece rotation angle is around the C-axis, the X- and Z- axes are utilized for movement along the face width, and the Y-axis is utilized for moving to the cutting location. The four-axis cutting coordinates for the pinion and gear

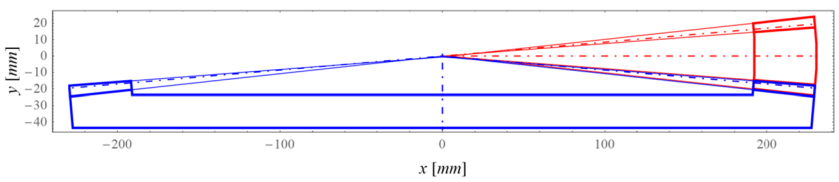

Fig. 7 Gear blanks of the example pair

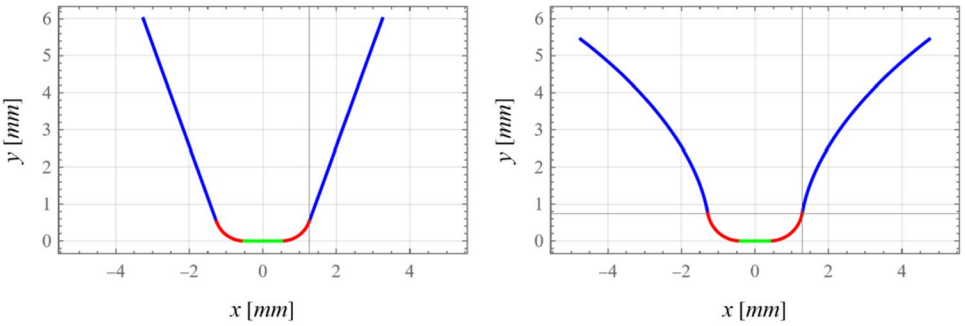

Fig. 8 Profiles of the disk cutters for both gears

(a) Tool profile of the ring gear

(b) Tool profile of the pinion

are converted from the universal machine settings and listed as Eqs. (10) and (11).

$$\begin{cases} x(s,\xi) = 0 \\ y(s,\xi) = \left(s + r_a\right)cos\delta_f + \left(\xi + \xi_0\right)sin\delta_f \\ z(s,\xi) = -\left(s + r_a\right)sin\delta_f + \left(s + r_a\right)cos\delta_f - M_d \end{cases} \tag{9}$$

$$\begin{cases} c_x(s,\xi) = z(s,\xi) \\ c_y(s,\xi) = y(s,\xi) \\ c_z(s,\xi) = 0, \psi_a(\xi) = 0 \end{cases} \tag{10}$$

$$\begin{cases} c_x(s,\xi) = y(s,\xi) \\ c_z(s,\xi) = -z(s,\xi) \\ c_y(s,\xi) = 0, \psi_c(\xi) = 0 \end{cases} \tag{11}$$

5 Corrected four-axis coordinates for cutting the pinion's tooth surface

When deriving the pinion's tooth surface, we utilize the profile at the gear's conjugate middle tooth surface to design the cutting tool. As a result, conjugation occurs exclusively in the middle of the teeth between two gears, given that the pinion is manufactured using the forming method. Figure 6a illustrates deviations δ_e between the pinion's tooth surface and the gear's conjugate surface, with negative errors toward the toe and positive errors toward the heel. Therefore, we must compensate for tooth surface errors to obtain a tooth surface that closes the conjugate tooth surface. Additionally, second-order crowning δ_c is applied in the tooth's longitudinal direction to absorb assembly and manufacturing errors, as shown in Fig. 6b.

The correction target δ_T is the sum of the error compensation $-\delta_e$ and the crowning amount δ_c for the pinion, as expressed in the following equation. These can be used to correct the cutting path further to obtain a better pinion tooth surface.

$$\delta_T = -\delta_e + \delta_c \tag{12}$$

Substituting $s = 0$ into Eq. (10), the initial cutting path of c_{x0} and c_{y0} can be obtained. Then, the third-order correction polynomials of the variable ξ are added to the four-axis motion as the following equation:

$$\begin{cases} c_x(\xi) = c_{x0}(\xi) + x_0 + x_1\xi + x_2\xi^2 + x_3\xi^3 \\ c_y(\xi) = c_{y0}(\xi) + y_0 + y_1\xi + y_2\xi^2 + y_3\xi^3 \\ c_z(\xi) = z_0 + z_1\xi + z_2\xi^2 + z_3\xi^3 \\ \psi_a(\xi) = a_0 + a_1\xi + a_2\xi^2 + a_3\xi^3 \end{cases} \tag{13}$$

where x_i, y_i, and z_i represent the coefficients for three translations, while a_i represents the coefficients for a workpiece rotation, and the subscript i indicates degrees ranging from 0 to 3.

If the target corrections $\{\delta D_i\}$ are provided, sensitivity analysis can be employed to determine the sensitivity matrix

Table 2 Partial data points of the pinion cutter profile

No	Right side		No	Left side	
	x[mm]	y[mm]		x[mm]	y[mm]
1	0.396	0	1	−0.396	0
3	0.704	0.054	3	−0.704	0.054
5	0.975	0.211	5	−0.975	0.211
7	1.176	0.451	7	−1.176	0.451
9	1.282	0.746	9	−1.282	0.746
11	1.45	1.393	11	−1.45	1.393
13	1.713	2.023	13	−1.713	2.023
15	2.059	2.636	15	−2.059	2.636
17	2.476	3.233	17	−2.476	3.233
19	2.958	3.812	19	−2.958	3.812
21	3.497	4.374	21	−3.497	4.374
23	4.093	4.919	23	−4.093	4.919
25	4.744	5.447	25	−4.744	5.447

$x = \pm\left(1.232 + 0.295u + 4.690u^2 - 2.115u^3 + 0.642u^4\right)$
$y = 0.302 + 5.715u - 0.390u^2 - 0.2642u^3 + 0.080u^4$

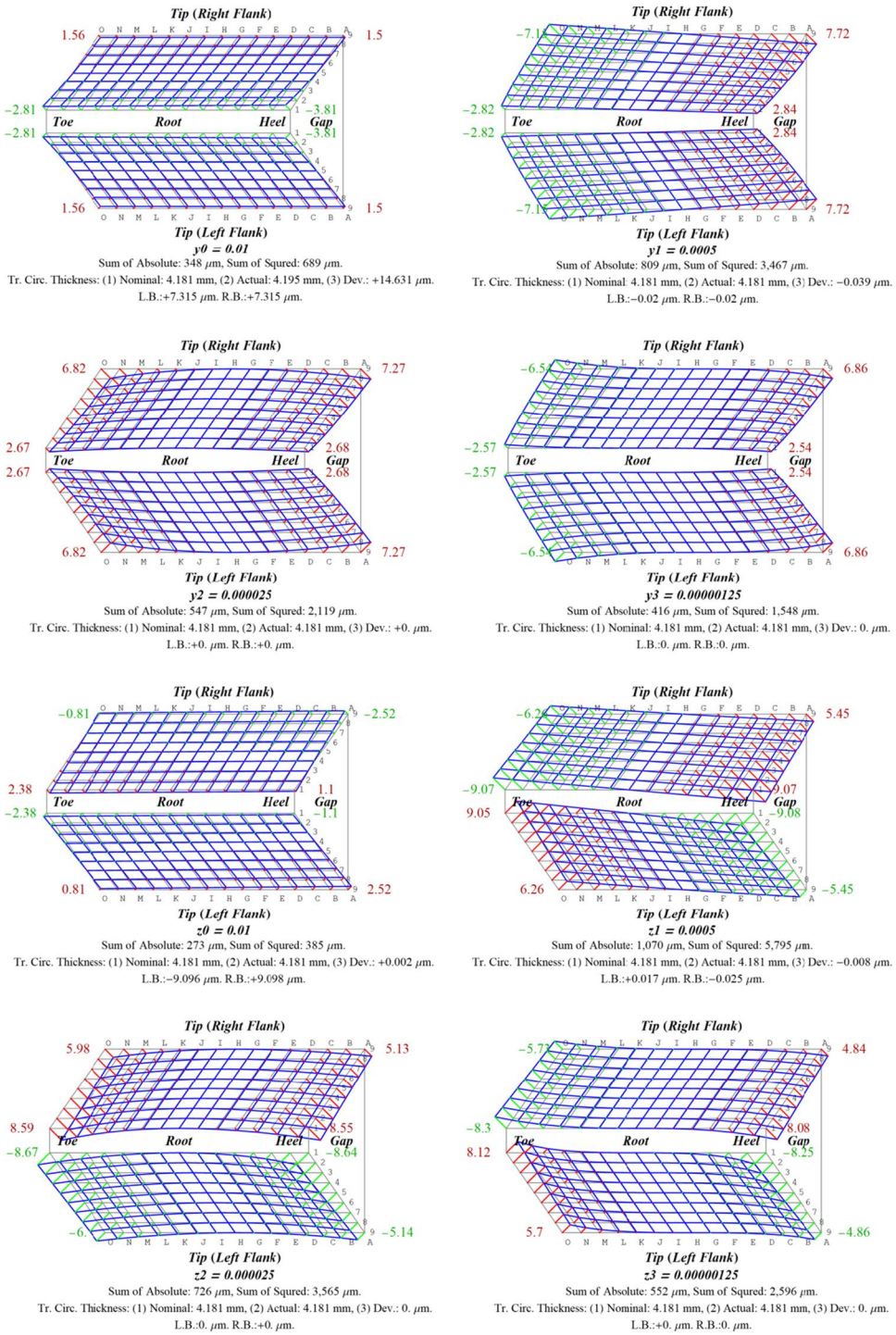

Fig. 9 Flank sensitivity topographies correspond to the selected coefficients of coordinates for the pinion

$[S_{ij}]$ of tooth surface topology points concerning the polynomial coefficients. The corrections to the polynomial coefficients $\{\delta a_j\}$ can be obtained using the least squares method through the following equation.

$$\{\delta a_j\} = \left([S_{ij}]^T [S_{ij}]\right)^{-1} [S_{ij}]^T \{\delta D_i\} \tag{14}$$

6 Numerical examples and discussion

The numerical example features a pair of SBGs with a high gear ratio employed in a scroll chuck for a turning machine. Their design parameters, gear blank parameters, and tool parameters are shown in Table 1. The gears have tooth numbers of 13 and 153, with a module of 3.0 mm. The tool diameters for the pinion and ring gear are 65 mm and 126

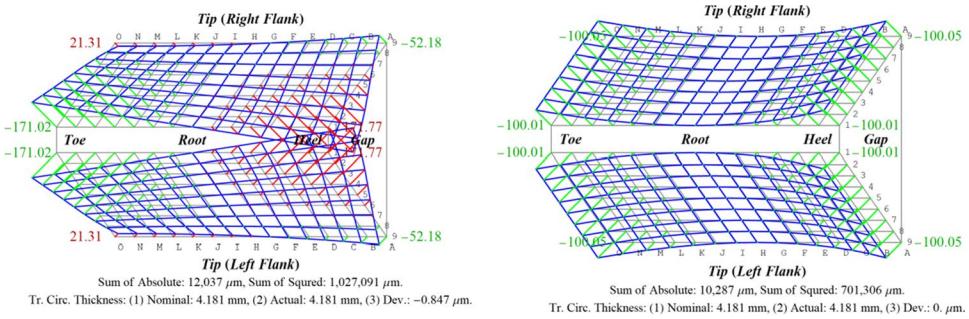

(a) Deviations compared with the conjugated flank

(b) Second-order flank crowning

Fig. 10 Flank deviation and crowning of the pinion tooth surface

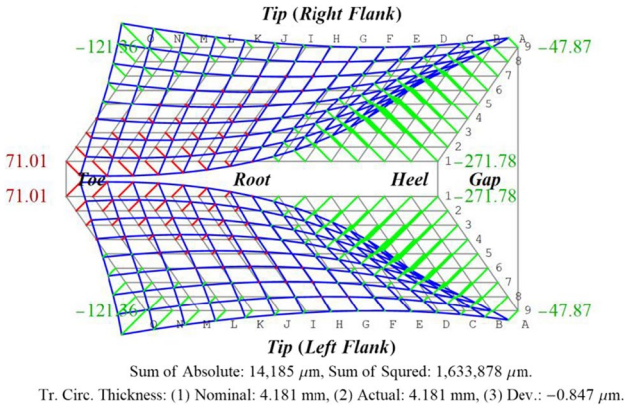

Fig. 11 Correction target of the pinion tooth surface

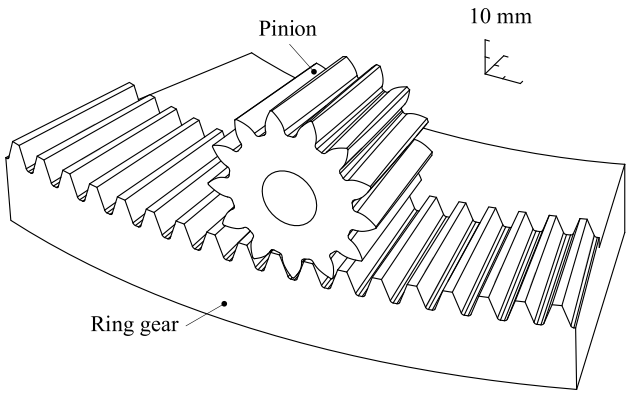

Fig. 12 3D model of the gears (created using SolidWorks)

mm, respectively, with initial point widths of 2.20 mm and 2.04. Based on the blank parameters, the gear blanks of the example are plotted and depicted in Fig. 7.

The tool for the ring gear is designed as a disk cutter with a straight edge and a fillet, illustrated in Fig. 8a. Using this tool to machine the gear tooth surface, and based on this, we derive the conjugate tooth surface. Subsequently, we can determine the tool profile for the pinion. In this case, a relief amount of 0.03 mm is applied to the tool profile of the pinion. The partial positions of tool profile points and their position equations can be found in Table 2, accompanied by the tool profile diagram shown in Fig. 8b. In the manufacturing process, the point width of the gear's tool is increased by 0.1 mm to achieve a backlash of 0.1 mm. Additionally, to prevent overcutting at the toe of the tooth surface, the point width of the pinion's tool is reduced by 0.5 mm.

Table 3 Four-axis cutting coordinates for both gears

Items	Pinion		Gear
(a) Universal settings			
r_a Radius of the cutter	32.500		63.000
δ_f Root angle	4.341°		83.886°
ξ_0 Initial distance	211.336		211.378
(b) Four-axis coordinates	$-22.000 \le \xi \le 22.000$		$-22.000 \le \xi \le 22.000$
	Design	Corrected	Design
c_x X axis	$-22.231+0.997\,\xi$	$-22.231+0.997\,\xi$	$216.885+0.994\,\xi$
c_y Y axis	$48.402+0.076\,\xi$	$48.402+8.811\times10^{-2}\xi - 1.610\times10^{-4}\xi^2 - 3.206\times10^{-7}\xi^3$	0.000
c_z Z axis	0.000	$\pm(0.250+1.436\times10^{-2}\xi + 2.479\times10^{-4}\xi^2 - 1.860\times10^{-7}\xi^3)$	$83.630-0.107\,\xi$
ψ_a Workpiece angle (°)	0.000	0.000	0.000

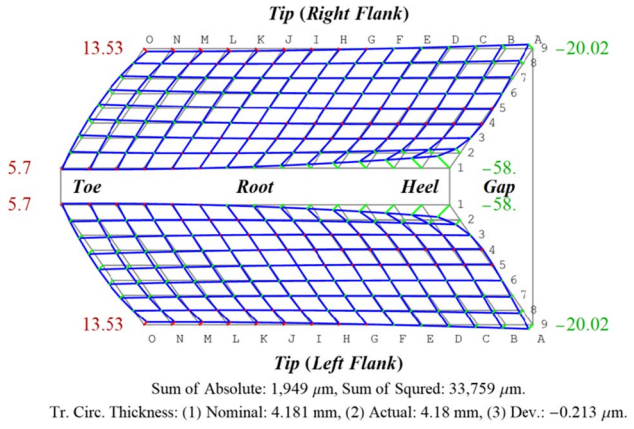

Fig. 13 Simulated flank topographic deviations of the pinion after correction

Sensitivity analysis is a common method to rectify tooth surface errors in gear manufacturing. A sensitivity matrix for machine settings in relation to tooth surface errors can be derived by systematically examining the influence of different machining machine settings on these errors. Following this, adjustments to the machine settings can be ascertained based on the desired correction amount for the tooth surface. In this case, it is essential to correct the cutting motion of the pinion to attain the desired tooth surface. In this context, our focus is solely on correcting the movement along the y and z machine axes. The flank sensitivity topographies of their polynomial coefficients for motion have been examined, and the findings are presented in Fig. 9. The coefficient $y0$ is associated with tooth profile direction error, $z0$ is related to diagonal direction error, and the remaining coefficients are associated with tooth face width direction error. These sensitivity topographies can be employed to construct the sensitivity matrix of coefficients for determining the corrections.

Figure 10a presents the deviation of the uncorrected pinion tooth surface compared to the conjugate tooth surface. Negative errors result in a clearance between the pinion and gear, while positive errors lead to interference between them. The maximum interferences at the toe and heel are 21.3 µm and 171.8 µm, respectively, with a tooth thickness error of −0.8 µm. Additionally, to mitigate assembly sensitivity, a second-order crowning amount of 100.0 µm is applied in the longitudinal direction of the pinion tooth surface, as depicted in Fig. 10b. The correction target is computed by reverse deviations adding corrections, and its result is illustrated in Fig. 11.

Once the sensitivity matrix and correction target are obtained, the correction amounts for motion coefficients can be determined according to Eq. (14). Adding these correction amounts to the initial coordinates results in the

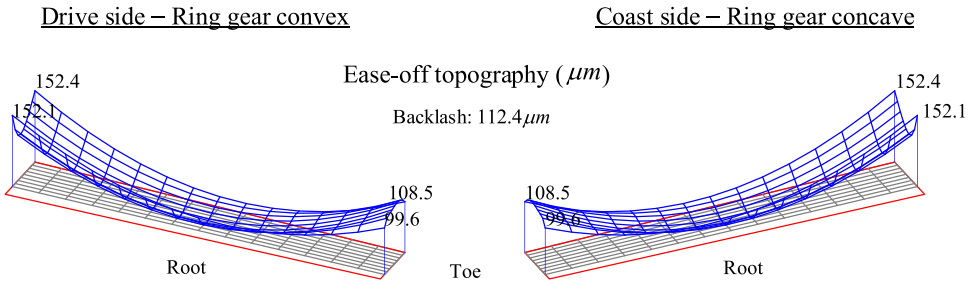

Fig. 14 Ease-off topography for the numerical example

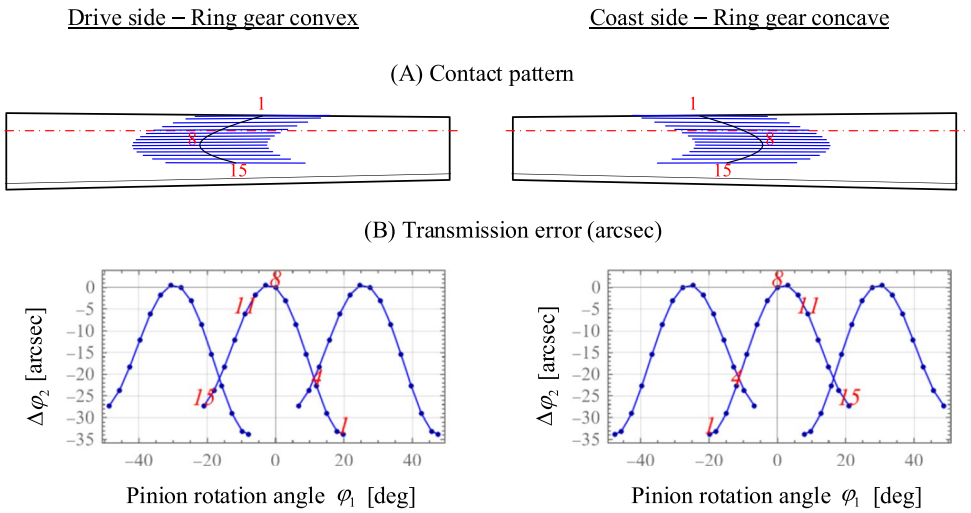

Fig. 15 Result of tooth contact analysis for the numerical example

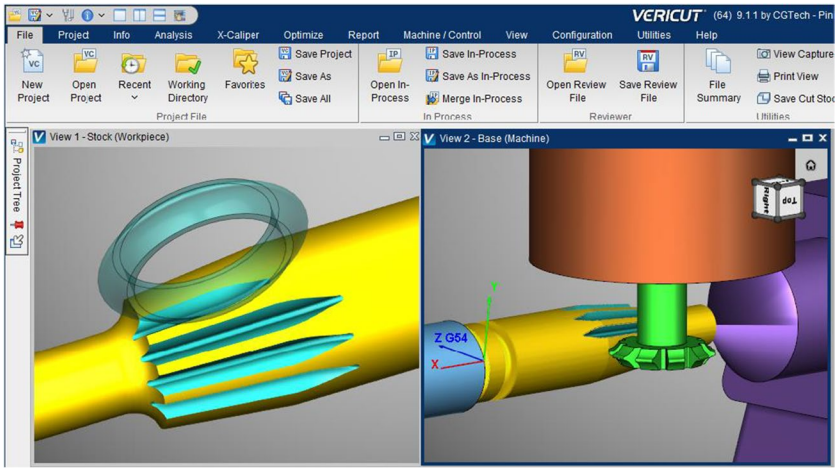

Fig. 16 Cutting simulation for the pinion using VERICUT

corrected machining positions for the pinion. The four-axis coordinates for producing both gears are determined and listed in Table 3. Substituting the cutting coordinates of the gears yields the tooth surfaces. The solved tooth surface points can be used to construct a 3D gear model, as illustrated in Fig. 12. The deviation between the final corrected tooth surface of the pinion and the target tooth surface is then investigated. The results are presented in Fig. 13. The maximum positive deviation in the tooth surface is + 13.5 μm, and the tooth thickness deviation is − 0.213 μm. Because of the originally designed 0.1-mm backlash, there will be no interference issues with the gears.

Figure 14 shows the ease-off topography for the numerical example. The ease-off has a maximum amount of 152.4 μm. All ease-off amounts are positive, indicating no interference between the pinion and gear, and are in point contact. Figure 15 illustrates the result of tooth contact analysis. The contact points are located in the middle of the tooth, and the tooth-bearing occupies approximately one-third of the tooth face width. The curves of angular transmission errors for three teeth intersect, indicating that vibration is not expected to occur. A maximum transmission angle error of 20.1 *arcsec* is quite reasonable for a bevel gear design.

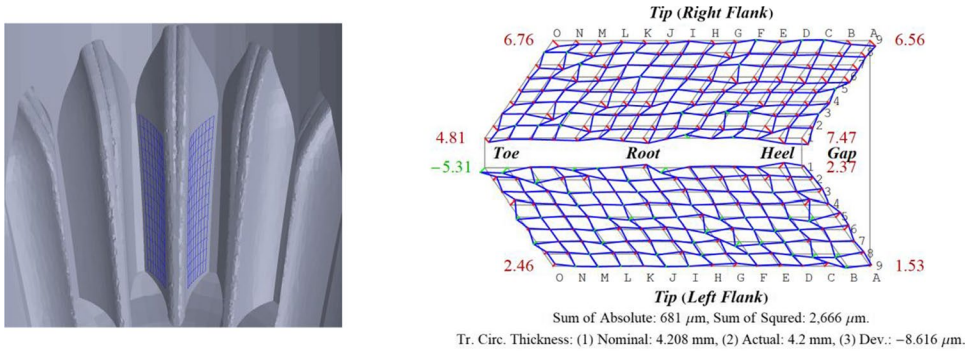

(a) Flank deviations of the pinion

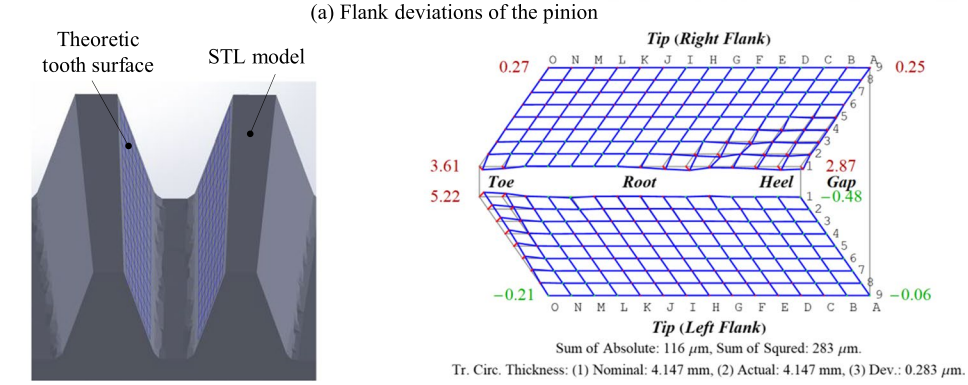

(b) Flank deviations of the ring gear

Fig. 17 Flank deviations of the simulated tooth surfaces by VERICUT compared to the theoretical tooth surfaces

Fig. 18 Photograph for the produced gear pair

The commercially available software, VERICUT, is used for gear-cutting simulation to eliminate NC program errors. Here, only the cutting simulation of the pinion is presented in Fig. 16. Using the tooth surface error analysis software developed by our lab, the simulated errors compared to the theoretical tooth surface were calculated. The results are shown in Fig. 17a for the pinion, with a maximum error of 7.47 μm and a tooth thickness error of − 8.616 μm. Figure 17b shows the results for the ring gear, with a maximum error of 5.22 μm and a tooth thickness error of + 0.283 μm. Both results validate the correctness of the NC program programming. Finally, we conducted cutting experiments on a four-axis CNC milling machine for the pinion and ring gear. Figure 18 shows the photograph of the completed gears. The tooth-bearing is very close to the target positions we designed.

7 Conclusions

This paper proposes an innovative mathematical model for the tooth surfaces of SBGs produced using the forming method. Such a model ensures a good contact performance between two gears. It also provides a feasible solution for mass-producing SBGs using a four-axis machine. In this study, with the ring gear as the reference gear, we derived the tool profile for the pinion along with its corresponding four-axis nonlinear cutting movement by considering the condition of point conjugate contact in a gear pair. Subsequently, two analysis methods, ease-off and tooth contact analysis, are employed to validate that the gear pair has a better contact performance. The final numerical control codes, generated based on the established mathematical model, underwent simulation using VERICUT software for the cutting process. The maximum tooth surface errors for the pinion and gear are determined to be 7.47 μm and 5.22 μm, respectively, while their tooth thickness errors were − 8.616 μm and + 0.283 μm. These results successfully confirm the accuracy of the NC codes. Once the design is finalized, it can be directly translated into manufacturing, significantly shortening the overall development time of SBGs using this cutting method. The machining approach can be implemented on a four-axis CNC machine tool, significantly reducing machine costs for manufacturers and enhancing their competitiveness.

Nomenclature c_x, c_y, c_z : Translating coordinates of the four-axis CNC milling machine; s : Cutting stock; u : Parameter of the cutting edge; ϕ_1, ϕ_2 : Rotation angles of the pinion and ring gear; ψ_a : Rotational coordinate of the four-axis CNC milling machine for producing the pinion; ψ_c : Rotational coordinate of the four-axis CNC milling machine for producing the ring gear; ξ : Infeed from toe to heel; $\mathbf{M}_{ij}$: Homogeneous transformation matrix from coordinate system S_j to coordinate system S_i; $\mathbf{r}_1$: Locus of the tool in the coordinate system S_1; $\mathbf{r}_g$: Locus of the ring gear tooth surface in the coordinate system S_1; $\mathbf{r}_1'$: Corrected profile of the pinion's tool; $\mathbf{r}_t$: Tool cutting edge in the coordinate system S_t; $\mathbf{R}_2$: Position of the ring gear's tooth surface; $\mathbf{R}_g$: Conjugate tooth surface of the ring gear; $\left[S_{ij}\right]$: Sensitivity matrix with respect to the coefficients of the polynomials for the four-axis motion; $\left\{\delta a_j\right\}$: Corrections of polynomial coefficients; $\left\{\delta D_i\right\}$: Target corrections

Acknowledgements The authors thank the National Science and Technology Council of the Republic of China (R.O.C.) and Yanmech Industrial Co. Ltd. for their financial support. This work was partially conducted under Contract No. MSTC 111-2221-E-011-098. Special thanks to Dr. Bor-Tyng Sheen and Mr. Jing Guo for their valuable efforts in revising the paper.

Author contribution All authors contributed to the study conception and design. Material preparation, data collection, and analysis were performed by Yi-Pei Shih and Guang-Yu Chen. The first draft of the manuscript was written by Yi-Pei Shih and all authors commented on previous versions of the manuscript. All authors read and approved the final manuscript.

Funding This work was supported by the National Science and Technology Council of the Republic of China (R.O.C.) (No. MSTC 111–2221-E-011–098). Author Yi-Pei Shih has received research support from Yanmech Industrial Co. Ltd.

Declarations

Competing interests The authors declare no competing interests.

References

1. The Gleason Works (1961) Calculating instructions generated straight bevel Coniflex® gears (No. 2A, 102, 104, 114 and 134 Straight Bevel Coniflex Generators). Rochester, NY, USA
2. Dudley DW (1962) Gear handbook, 1st edn. McGraw-Hill, New York
3. Yoshida M, Suetomi T (1987) The mechanism of straight-bevel gear cutting by a circular-type cutter. Bull Jpn Soc Precis Eng 21(4):301–302
4. Ichino K, Tamura H, Kawasaki K (1996) Method for cutting straight bevel gears using quasi-complementary crown gears. ASME Des Eng Div 88:283–288

5. Chang CK, Tsay CB (2000) Mathematical model of straight bevel gears with octoid form. J Chin Soc Mech Eng 21(3):239–245
6. Özel C, Ian A, Özler L (2005) An investigation on manufacturing of the straight bevel gear using end mill by CMC milling machine. ASME J Manuf Sci Eng Trans 127(3):503–511
7. Tsuji I, Kawasaki K, Gunbara H, Houjoh H, Matsumura S (2013) Tooth contact analysis and manufacture on multi-tasking machine of large-sized straight bevel gears. ASME J Mech Des 135(3):034504 (8 pages)
8. Wang P (2020) An envelope shaping method for huge straight bevel gear. SN Appl Sci 2(1):133
9. Stadtfeld HJ (2007) Straight bevel gear cutting and grinding on CNC free form machines. AGMA Fall Technical Meeting, Detroit, MI, Oct. 7–9, Paper No. 07FTM16
10. Zhang M, Li H, Wei D (2011) Numerical control innovation for double cradle straight bevel gear milling machine. Proc Procedia Eng 15:1149–1153
11. Shih YP, Hsieh HY (2016) Straight bevel gear generation using the dual interlocking circular cutter cutting method on a computer numerical control bevel gear-cutting machine. ASME J Manuf Sci Eng Trans 138(2):021007 (11 pages)
12. Shih YP, Hung YC, Sheen BT, Chen SH, Lin KH (2022) Mathematical model of a straight bevel gear on the straight bevel Coniflex generator and gear flank correction. Proc. American Gear Manufacturers Association Fall Technical Meeting
13. Fuentes-Aznar A, Yague-Martinez E, Gonzalez-Perez I (2018) Computerized generation and gear mesh simulation of straight bevel gears manufactured by dual interlocking circular cutters. Mech Mach Theory 122:160–176
14 Shih YP (2012) Mathematical model for face-hobbed straight bevel gear. ASME J Mech Des 134(9):091006 (11 pages)
15. Shih YP, Huang YC, Lee YH, Wu JM (2013) Manufacture of face-hobbed straight bevel gears using a six-axis CNC bevel gear cutting machine. Int J Adv Manuf Technol 68:2499–2515
16. Li J, Meng W, Shi J (2012) Preliminary study on the rotational indexing machining technology of straight bevel gear. Proc Appl Mech Mater 217–219:1650–1654
17. Litvin FL, Fuentes A (2004) Gear geometry and applied theory, Chap. 6, 2nd edn. Cambridge University Press, Cambridge, UK